IEEE Access
Multidisciplinary | Rapid Review | Open Access Journal

Received July 14, 2019, accepted August 8, 2019, date of publication August 14, 2019, date of current version August 28, 2019.

Digital Object Identifier 10.1109/ACCESS.2019.2935218

Low-Complexity Energy-Efficient Power Allocation With Buffer Constraint in HSR Communications

XIAOMING WANG[1,2], (Member, IEEE), MI YU[1], JINLING HU[1], AND YOUYUN XU[1], (Senior Member, IEEE)

[1]College of Telecommunication and Information Engineering, Nanjing University of Posts and Telecommunications, Nanjing 210003, China
[2]National Mobile Communications Research Laboratory, Southeast University, Nanjing 210096, China

Corresponding author: Xiaoming Wang (xmwang@njupt.edu.cn)

This work was supported in part by the National Key Research and Development Program of China under Grant 2016YFE0200200, in part by the National Natural Science Foundation of China under Grant 61801240, Grant 61601243, and Grant 61772287, in part by the Natural Science Foundation of the Jiangsu Providence under Grant BK20180753, in part by the Natural Science Foundation of the Jiangsu Higher Education Institutions of China under Grant 17KJB510046, and in part by the Open Research Fund of the National Mobile Communications Research Laboratory, Southeast University, under Grant 2019D16.

ABSTRACT In this paper, we investigate the energy-efficient power allocation for downlink distributed antenna system (DAS) with buffer size constraint in high-speed railway (HSR) scenarios. We design the power allocation at different times for HSR communications, utilizing the characteristics of fixed moving path of trains. A key issue we discuss is the matching problem between the data arrival process and instantaneous wireless transmission process under the buffer size constraint. We formulate the energy-efficient power allocation problem with the requirement of buffer size as a non-convex optimization problem. By a parameterized transformation and an iterative algorithm, we derive the optimal solution at different time phases. Then, to reduce complexity of the multiple iterations, we present a low-complexity algorithm by analyzing the feasible region of the optimal solution. Simulation results demonstrate that the proposed power allocation schemes can achieve the optimal energy efficiency (EE) and avoid data overflow. Moreover, with a smaller number of iterations, the low-complexity algorithm can achieve the same EE performance as the optimal algorithm based on the bisection method.

INDEX TERMS Power allocation, buffer constraint, low-complexity, high-speed railway, energy efficiency.

I. INTRODUCTION

High-speed railway (HSR) has been becoming more and more popular with people for its superiority such as high mobility, time saving and reliability. Meanwhile, the demands for broadband services and applications in HSR are growing strictly, and the quality-of-service (QoS) requirements of information transmission have significantly increased [1]. However, they lead to high power consumption, which is inconsistent with the development trend of green communications [2], [3]. Particularly, the HSR has been a high energy-consuming industry. The high power cost restricts the sustainable development of the railways and leads to serious environmental problems [4]–[6]. Therefore, energy efficiency (EE) has become an important issue for HSR communications due to its profits of the economy and society [7]–[9].

In HSR communications, a two-hop relay architecture is usually adopted to combat the serious penetration loss of carriages. Base station (BS) communicates with the passengers in the train through mobile relays (MRs) on the train [10]. In the hop from the BS and the MRs, severe large-scale fading and Doppler spread bring special challenges for efficient utilization of radio resources. A practical solution to these challenges is to dynamically optimize the allocation of power on the basis of channel states along with the railway. For instance, Xiong *et al.* in [11] presented a power allocation method to achieve the tradeoff between the proportional and water-filling power allocations. Li *et al.* in [12] derived the optimal power allocation and obtained the largest achievable

The associate editor coordinating the review of this article and approving it for publication was Sohail Jabbar.

rate region for hybrid streams with diverse QoS demands. Ahmad *et al.* in [13] investigated the co-channel interference management and resource allocation for coexistence of public safety and railway networks based on the performance metrics of throughput, interference and outage. Particularly, for orthogonal frequency division multiple access (OFDMA) system in HSR communications, some work of resource allocation has been done [14]–[18]. Among the research work, Qiu *et al.* in [14] studied a joint subcarrier pairing, subcarrier assignment and power allocation in HSR communications with the inter-carrier interference. Zhang *et al.* in [15] investigated the resource allocation problem for OFDMA HSR systems coexisting with local users. Sheng *et al.* in [16] proposed a power allocation scheme between pilot and data symbols which achieved a trade-off between channel estimation and data transmission in HSR scenarios. Gao *et al.* in [17] proposed an adaptive modulation and power allocation scheme to maximize normalized average throughput of the HSR system. Ghazzai *et al.* in [18] proposed a resource allocation scheme to minimize the total power consumption and presented a planning method to optimally determine the inter-BS distance according to given QoS parameters.

Additionally, adopting multiple antennas at both transmitter side and receiver side in the HSR communication system, has been recognized as a good way to improve the transmission rate and the EE performance. Wang *et al.* in [7] studied the millimeter wave communication with directional beamforming in HSR, and they proposed an energy-efficient power control scheme with a power minimization algorithm. Zhao *et al.* in [19] and [20] proposed joint resource allocations of subcarriers, antennas, time slots and power in downlink multi-antenna OFDM HSR communication system, to minimize total transmit power and maximize throughput respectively. Literatures [21] and [22] investigated beamforming schemes to maximize the information transmission rate for the HSR scenarios of co-existing low-mobility users and encountering trains respectively. And in [23] and [24], the authors studied the angle-domain Doppler shifts compensation and beam tracking scheme, considering massive multiple-input multiple-output (MIMO) in HSR scenarios. Particularly, distributed antenna system (DAS) that is a promising multi-antenna architecture based on radio over fiber, can further increase throughput and avoid frequent handover [25]–[28]. In DAS, remote access units (RAUs) are geographically distributed in cells (or along with railways) and connected to baseband processing unit via optical fiber or cable, which can reduce the access distances between the mobile stations (or trains) and BS. Literatures [29] and [30] studied the power allocation problem on maximizing EE and the trade-off relation between the EE and spectral efficiency in DAS. For HSR, Liu *et al.* in [31] proposed an effective handover scheme in DAS for ground-train communication. In [32] and [33], the authors investigated the HSR communication system with distributed RAUs and proposed joint optimal power allocation and antenna selection methods.

However, most of the existing works are insufficient in considering the matching problem of the data arrival process and wireless transmission process. We know that the channels between the RAUs and the MRs are time-varying, so the wireless channel service ability and the data arrival process may be always different, i.e., mismatching. When the trains move to some positions, channel conditions may be able to support the transmission of the arrival data well enough, but at other positions they may not be. Fortunately, the trains run only on the rails and the channels change regularly. If setting a data buffer in the central unit (CU), we can design the power allocation to optimize the performance of HSR communication with a tolerable delay of users. In [34], Zafer and Modiano studied a rate control policy to minimize the total energy expenditure over a time-varying channel, where they considered a deadline-constrained transmission similar to the matching problem. Literatures [35] and [36] proposed power optimization schemes in uplink HSR communication system, and considered the buffer constraint at the access point by matching data arrival process and wireless transmission process under single-antenna point-to-point communication. However, the study of the power allocation with the matching problem in the multi-antenna HSR communication system has not been appeared in existing literatures.

In this paper, we propose an optimal power allocation scheme to achieve maximum EE of downlink DAS in HSR communications with buffer constraint. We first analyze the dynamic matching process of data arrival and wireless transmission at the CU and formulate a power optimization problem based on the analysis. Then, to solve the formulated non-convex optimization problem, we present a transforming method and an iterative algorithm. Based on this, we can obtain the energy-efficient optimal power allocation scheme under the buffer constraint. In addition, we analyze the all cases of the optimal solution in feasible region of constraints, and propose a low-complexity power allocation algorithm.

The main contributions of this paper can be summarized as follows:

- We formulate the energy-efficient power allocation problem in the multi-antenna HSR communication system with buffer constraint as a non-convex optimization problem.
- We derive the energy-efficient optimal power allocation in different time phases as the movement of the high-speed train. Meanwhile, it ensures the matching of the data arrival process and wireless transmission process.
- We propose a low-complexity energy-efficient power allocation algorithm which can achieve the same performance to the optimal method.

The rest of this paper is organized as follows. Section II introduces the system model and formulates the energy-efficient power allocation problem. Section III proposes the transforming method and the iterative algorithm to solve the optimization problem. In Section IV, we discuss

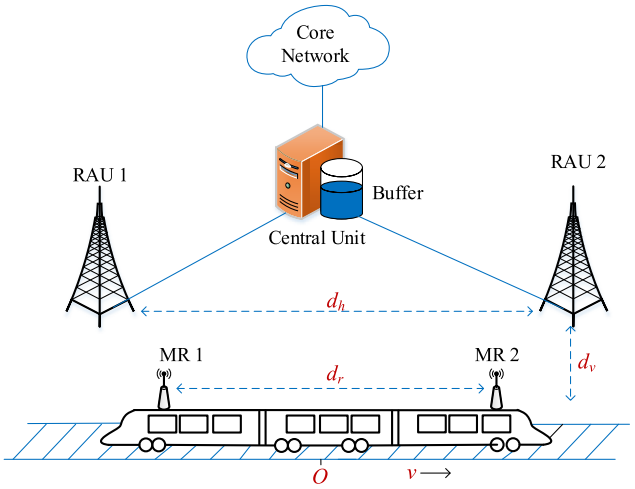

FIGURE 1. Two-hop architecture system model with distributed antenna in the HSR scenario.

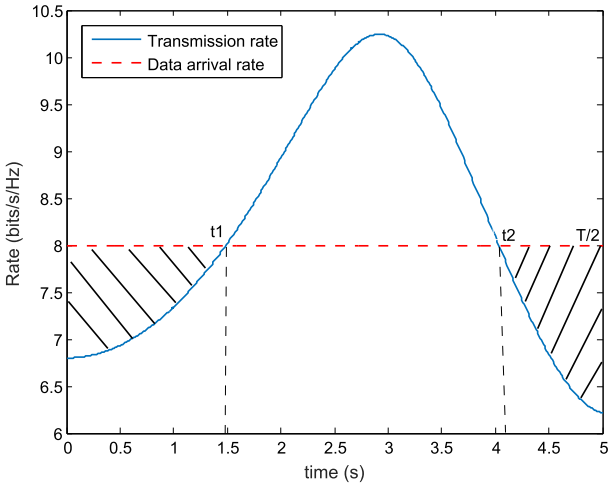

FIGURE 2. Instantaneous wireless transmission rate and constant data arrival rate, where $v = 100$ m/s, $d_h = 1000$ m, $d_v = 100$ m, $d_r = 400$ m, $\alpha = 3.6$, $u = 8$ bits/s/Hz, $P = 30$ W.

the optimal solution cases and provide the low-complexity algorithm. Section V presents the simulation results. Finally, we draw the conclusions in section VI.

II. SYSTEM MODEL AND PROBLEM FORMULATION

A. SYSTEM MODEL

We consider a downlink HSR mobile communication system, where the RAUs are positioned along the railway and connected to the central unit by optical fibers [26], [27]. As shown in Fig. 1, two RAUs are responsible for the communication between the core Internet and the train in each cell. The CU with data buffer sends signals to corresponding RAUs, and then the RAUs transmit signals to MRs installed on the carriage.

Suppose that d_h is the horizontal distance between two adjacent RAUs, d_v is the vertical distance from RAUs to the railway line and d_r is the distance between MRs. Let d_{ij} denote the distance between RAU i and MR j. Assume that the train moves with uniform speed of v, and the time is zero (i.e., beginning of the time period) when the train moves to the point O located at the middle of two RAUs as shown in Fig. 1. Since the distance between MRs and RAUs is symmetrical about O and then the path loss between the two is periodic, we only need to design power allocation scheme in half of a period, i.e. $t \in [0, \frac{T}{2}]$, where t is the time index and $T = d_h/v$.

Since most HSR scenarios are viaducts (occupying more than 70%), the impact of large-scale fading far exceeds small-scale fading. Thus, we focus on the path-loss in this paper. The small-scale fading will be tested in simulations. The channel gain at time t between the RAU$_j$ and MR$_i$ is expressed as

$$h_{ij}(t) = \left(\left(\frac{d_h - (-1)^{i+j} d_r}{2} - (-1)^i vt\right)^2 + d_v^2\right)^{-\frac{\alpha}{2}}, \quad (1)$$

where α is the path-loss exponent. The channel fading matrix of system is

$$\mathbf{H}(t) = \begin{bmatrix} h_{11}(t) & h_{12}(t) \\ h_{21}(t) & h_{22}(t) \end{bmatrix}. \quad (2)$$

Denote total transmit power of the system at time t as $P(t)$ and transmit power of each RAU as $\frac{P(t)}{2}$. Thus the corresponding instantaneous channel capacity can be expressed as

$$C(t) = \log_2 \det\left(\mathbf{I} + \frac{1}{N_0}\begin{bmatrix} P(t)/2 & 0 \\ 0 & P(t)/2 \end{bmatrix} \mathbf{H}^T(t)\mathbf{H}(t)\right), \quad (3)$$

where N_0 is the noise power, $\mathbf{I}$ denotes the identical matrix, $(\cdot)^T$ and $\det(\cdot)$ represent the conjugate transpose and determinant of $(\cdot)$, respectively. Substituting (1) into (3), the system capacity is rewritten as

$$C(t) = \log_2\left(1 + \frac{A(t)P^2(t)}{4N_0^2} + \frac{B(t)P(t)}{2N_0}\right), \quad (4)$$

where

$$A(t) = (h_{11}(t)h_{22}(t) - h_{21}h_{12}(t))^2, \quad (5)$$

$$B(t) = \sum_{i=1}^{2}\sum_{j=1}^{2} h_{i,j}^2. \quad (6)$$

The data arrival rate at the CU is denoted by u, which is simplified as a constant. When the channel condition is worse, the instantaneous wireless transmission rate is less than the arrival rate, then there will be data buffering. We take the case where the RAUs transmit with constant power P as an example. From Fig. 2, we can see that the total channel gain between RAUs and MRs becomes better at first and then worse. Furthermore, the instantaneous wireless transmission rate is less than u in the time periods $[0, t_1]$ and $(t_2, \frac{T}{2}]$. Then it will be data buffering, while the cached data will gradually be transmitted all over because the instantaneous wireless

transmission rate is larger than u from t_1 to t_2. To avoid data overflow and infinite delay during the time period [35], the buffer size should satisfy

$$\frac{Q_m}{2} \geq \int_0^{t_1} (u - C(t))\mathrm{d}t + \int_{t_2}^{\frac{T}{2}} (u - C(t))\mathrm{d}t, \tag{7}$$

where Q_m denotes the buffer size. t_1 is the time that the transmission rate begins to be larger than the data arrival rate, while t_2 represents the cached point that it begins to store data again.

B. ENERGY EFFICIENCY OPTIMIZATION PROBLEM FORMULATION

Improving EE is a concern point for the design of wireless communication system in HSR scenarios, which plays an important role in green communications. The EE is usually defined as the average data volume transmitted per unit of energy consumption [9], [29], [30], [36]–[38]. The total power consumption in a DAS can be expressed as [30],

$$P_{total} = P_t + P_c = P_t + 2P_d + P_b + P_o, \tag{8}$$

where P_t is the radio frequency power consumption, i.e. $\int_0^{\frac{T}{2}} P(t)\mathrm{d}t$ in this paper. P_c is constant power consumption at CU and RAUs, consisting of the circuit power P_d of each RAU, the basic power P_b and the power dissipated by the optical fiber transmission P_o respectively.

However, the constant power allocation may not be the most energy-efficient scheme. Moreover, as shown in Fig. 2, the constant power allocation can not always meet the buffer size constraint, because a lot of data will be cached during $0 \leq t \leq t_1$ and $t_2 < t \leq \frac{T}{2}$. We aim to maximize the EE of the HSR system while satisfying the buffer constraint of CU by an appropriate power control. Therefore, the optimization problem in the downlink HSR system can be formulated as

$$\max_{P(t)} \frac{\int_0^{\frac{T}{2}} C(t)\mathrm{d}t}{\int_0^{\frac{T}{2}} P(t)\mathrm{d}t + P_c}, \tag{9a}$$

$$\text{s.t.} \ \frac{2}{T}\int_0^{\frac{T}{2}} P(t)\mathrm{d}t \leq P_{max}, \tag{9b}$$

$$\frac{2}{T}\int_0^{\frac{T}{2}} C(t)\mathrm{d}t \geq u, \tag{9c}$$

$$\int_0^{t_1} (u - C(t))\mathrm{d}t + \int_{t_2}^{\frac{T}{2}} (u - C(t))\mathrm{d}t \leq \frac{Q_m}{2}, \tag{9d}$$

where P_c is a constant power consumption at RAUs and CU given by (8). Constraint (9b) is the average transmit power constraint of RAUs. Constraint (9c) means that the average wireless channel capacity is no less than the data arrival rate u in order to avoid infinite delay. Constraint (9d) shows that the total amount of cached data can not exceed the buffer size in the time period $[0, \frac{T}{2}]$, otherwise it will lead to data overflow and loss. t_1 and t_2 are the time points of consuming and accumulating cached data. t_1 is the point based on optimal power allocation at which the $C(t)$ is no less than the u. And t_2 is the point based on optimal power allocation where the buffer begins to store data again. Obviously, this optimization problem is a non-convex problem with multiple constraints.

III. OPTIMAL ENERGY-EFFICIENT POWER ALLOCATION IN HSR WITH BUFFER CONSTRAINT

The optimization problem (9a)-(9d) is a non-linear fractional program. We can transform it into a parametric optimization problem with a more tractable non-fractional form as

$$\max_{P(t)} \int_0^{\frac{T}{2}} C(t)\mathrm{d}t - r\left(\int_0^{\frac{T}{2}} P(t)\mathrm{d}t + P_c\right)$$
$$\text{s.t. (9b)} - \text{(9d)}, \tag{10}$$

where r is an introduced auxiliary parameter for transforming the original problem. It can be computed by Dinkelbach method or the bisection method [37]. Problem (10) is convex with respect to $P(t)$ for a given r. We can adopt Lagrangian dual method to obtain its optimal solution. The Lagrangian function is

$$\begin{aligned}
&\mathcal{L}^{\mathrm{OPT}}(P(t), \lambda, \eta, \kappa) \\
&= -\int_0^{\frac{T}{2}} C(t)\mathrm{d}t + r\left(\int_0^{\frac{T}{2}} P(t)\mathrm{d}t + P_c\right) \\
&\quad + \lambda\int_0^{\frac{T}{2}} (P(t) - P_{ave})\mathrm{d}t - \eta\int_0^{\frac{T}{2}} (C(t) - u)\mathrm{d}t \\
&\quad - \kappa\int_0^{t_1} \left(C(t) - u + \frac{Q_m}{2t_1}\right)\mathrm{d}t - \kappa\int_{t_2}^{\frac{T}{2}} (C(t) - u)\,\mathrm{d}t.
\end{aligned} \tag{11}$$

From (11), we divide the power allocation during the time period into three phases. Since channel condition becomes better gradually and then worsen from the time period [0, $\frac{T}{2}$], the instantaneous channel capacity $C(t)$ may be less than the data arrival rate u in the first phase and the third phase. To avoid the data loss, it must be ensure that the amount of data buffered in these two phases should be less than the buffer size at the CU.

In the first phase from 0 to t_1, we have

$$\begin{aligned}
\mathcal{L}_1^{\mathrm{OPT}} &= (r + \lambda)\int_0^{t_1} P(t)\mathrm{d}t \\
&\quad - (1 + \eta + \kappa)\int_0^{t_1} C(t)\mathrm{d}t + Cons,
\end{aligned} \tag{12}$$

where $Cons$ means a constant independent of $P(t)$. Deriving (12) with respect to $P(t)$ and making the result be zero, we have

$$\frac{\partial \mathcal{L}_1^{\mathrm{OPT}}}{\partial P(t)} = r + \lambda - (\eta + \kappa)\frac{\partial C(t)}{\partial P(t)} = 0, \tag{13}$$

where

$$\frac{\partial C(t)}{\partial P(t)} = \frac{2A(t)P(t) + 2B(t)N_0}{(A(t)P^2(t) + 2B(t)P(t)N_0 + 4N_0^2)\ln 2}. \tag{14}$$

Thus, the optimal solution for power allocation for a given r during this period can be given by

$$P_1^{\mathrm{OPT}}(t) = \frac{2N_0^2}{(r+\lambda)A(t)}\left(\Theta_1^{\mathrm{OPT}}(t) + \sqrt{\Theta_1^{\mathrm{OPT}}(t))^2 - \Phi_1^{\mathrm{OPT}}(t) + \Omega_1^{\mathrm{OPT}}(t)}\right), \quad (15)$$

where

$$\Theta_1^{\mathrm{OPT}}(t) = \frac{(1+\eta+\kappa)A(t) - (r+\lambda)B(t)N_0\ln 2}{2N_0^2\ln 2}, \quad (16)$$

$$\Phi_1^{\mathrm{OPT}}(t) = \frac{A(t)(r+\lambda)^2}{N_0^2}, \quad (17)$$

$$\Omega_1^{\mathrm{OPT}}(t) = \frac{(r+\lambda)(1+\eta+\kappa)A(t)B(t)}{2N_0^3\ln 2}. \quad (18)$$

The parameters λ, η and κ are the Lagrange multipliers corresponding to the constraints of power consumption, average rate and buffer size respectively. Note that, these Lagrange multipliers need to be computed to guarantee global constraints in $[0, \frac{T}{2}]$ but not in any single phase. They can be computed by the bisection method or the subgradient method iteratively [39].

In the second phase $t_1 < t \le t_2$, $c(t)$ should be no less than u since the wireless channel condition is better than that in the rest two phases. Therefore, for the second phase, we get

$$\mathcal{L}_2^{\mathrm{OPT}} = (r+\lambda)\int_{t_1}^{t_2} P(t)\mathrm{d}t - (1+\eta)\int_{t_1}^{t_2}\eta C(t)\mathrm{d}t + Cons. \quad (19)$$

Similar to the first phase, deriving the (19) with respect to $P(t)$ and setting the result be zero, we have

$$\frac{\partial \mathcal{L}_2^{\mathrm{OPT}}}{\partial P(t)} = (r+\lambda) - (1+\eta)\frac{\partial C(t)}{\partial P(t)} = 0. \quad (20)$$

Substituting (14) into (20), the optimal power allocation with a given r in the second phase is

$$P_2(t) = \frac{2N_0^2}{(r+\lambda)A(t)}\left(\Theta_2^{\mathrm{OPT}}(t) + \sqrt{\Theta_2^{\mathrm{OPT}}(t))^2 - \Phi_1^{\mathrm{OPT}}(t) + \Omega_2^{\mathrm{OPT}}(t)}\right), \quad (21)$$

where

$$\Theta_2^{\mathrm{OPT}}(t) = \frac{(1+\eta)A(t) - (r+\lambda)B(t)N_0\ln 2}{2N_0^2\ln 2}, \quad (22)$$

$$\Omega_2^{\mathrm{OPT}}(t) = \frac{(r+\lambda)(1+\eta)A(t)B(t)}{2N_0^3\ln 2}. \quad (23)$$

Since $C(t) \ge u$ for $t_1 < t \le t_2$, we have

$$P_2^{\mathrm{OPT}}(t) = \max\left\{P_2(t), P_{th}(t)\right\}, \quad (24)$$

where

$$P_{th}(t) = \frac{2N_0^2}{A(t)}\left[\sqrt{\frac{B^2(t)}{4N_0^2} + \frac{A(t)(2^u-1)}{N_0^2}} - \frac{B(t)}{2N_0}\right]. \quad (25)$$

The optimal power allocation for the third phase is similar to the first phase, so

$$P_3^{\mathrm{OPT}}(t) = P_1^{\mathrm{OPT}}(t), \quad t_2 < t \le \frac{T}{2}. \quad (26)$$

In summary, the optimal power allocation for a given r is

$$P^{\mathrm{OPT}*}(t) = \begin{cases} P_1^{\mathrm{OPT}}(t), & 0 \le t \le t_1, \\ P_2^{\mathrm{OPT}}(t), & t_1 < t \le t_2, \\ P_3^{\mathrm{OPT}}(t), & t_2 < t \le \frac{T}{2}, \end{cases} \quad (27)$$

where t_1 and t_2 should satisfy

$$\int_0^{t_1} C^*(t)\mathrm{d}t + \int_{t_2}^{\frac{T}{2}} C^*(t)\mathrm{d}t \ge \left(t_1 + \frac{T}{2} - t_2\right)\frac{uQ_m}{2}, \quad (28)$$

and

$$\lim_{t\to t_1} C^*(t) = u, \quad \lim_{t\to t_2} C^*(t) = u. \quad (29)$$

We determine t_1 and t_2 using the following method. First, assuming there exist t_1 and t_2, we compute the power allocation in three phases as $P_1^{\mathrm{OPT}}(t)$, $P_2^{\mathrm{OPT}}(t)$ and $P_3^{\mathrm{OPT}}(t)$. From the expressions of $P_1^{\mathrm{OPT}}(t)$, $P_2^{\mathrm{OPT}}(t)$ and $P_3^{\mathrm{OPT}}(t)$, we note that their main difference is with different Lagrange multipliers corresponding to the buffer constraint. That is, the buffer constraint exists only during $[0, t_1]$ and $(t_2, \frac{T}{2}]$. This is because the cached data in buffer cumulatively increases in the two periods of time. And the cached data decreases from t_1 to t_2. Second, according to the form of the optimal solutions, we can obtain the form of optimal $C^*(t)$, although we do not get the value of t_1 and t_2 yet. Third, we compare instantaneous $C^*(t)$ with data arrival rate u. We obtain t_1 by $\lim_{t\to t_1^-} C^*(t) = u, \forall t$, where $t \to t_1^-$ means t approaches t_1 from $t < t_1$. It is the starting time point of consuming cached data. And we obtain t_2 by $\lim_{t\to t_2^+} C^*(t) = u, \forall t$, where $t \to t_2^+$ means t approaches t_2 from $t > t_2$. It is the starting time point of accumulating cached data again. Our proposed algorithm is based on the position of train, so we can compute the optimal power allocation and obtain t_1 and t_2 before the train moving into the coverage area, if the train moves with a uniform speed.

We provide an iterative algorithm as shown in Algorithm 1, to compute the auxiliary parameter r and get the optimal energy-efficient power allocation. We update r based on the bisection method, and

$$F(r) = \max_{P(t)}\left\{\int_0^{\frac{T}{2}} C(t)\mathrm{d}t - r\left(\int_0^{\frac{T}{2}} P(t)\mathrm{d}t + P_c\right)\right\}. \quad (30)$$

IV. LOW-COMPLEXITY ENERGY-EFFICIENT POWER ALLOCATION IN HSR COMMUNICATIONS

In the Section III, we have obtained an optimal power allocation by solving the transformed problem (10) and achieved the maximum EE by the iterative algorithm. However, Algorithm 1 needs multiple iterations where the introduced auxiliary parameter r is updated in outer iteration

Algorithm 1 Energy-Efficient Power Allocation Algorithm in HSR Communications With Buffer Constraint

Initialization

1. Initialize tolerance ε and index $n = 1$.
2. Initialize $r_d^{(0)}$ and $r_u^{(0)}$ with $F(r_d^{(0)}) > 0$ and $F(r_u^{(0)}) < 0$.

Iterative Algorithm

3. **repeat**
4. Update r by $r^{(n)} = (r_d^{(n-1)} + r_u^{(n-1)})/2$.
5. Compute $P(t)$ for the given $r^{(n)}$ by (27).
6. **if** $F(r^{(n)}) > 0$
7. Update $r_d^{(n)} = r^{(n)}$ and $r_u^{(n)} = r_u^{(n-1)}$;
8. **else**
9. Update $r_d^{(n)} = r_d^{(n-1)}$ and $r_u^{(n)} = r^{(n)}$;
10. **endif**
11. Set $n = n + 1$;
12. **endwhile** converge to the optimal $P^*(t)$ with ε.

and the Lagrangian multipliers (i.e., the dual variables) are updated in inner iterations, which leads to a high computational complexity. In this section, we discuss the feasible region of the optimal solution, and based on it we propose a low-complexity algorithm to obtain the optimal power allocation.

A. FEASIBLE REGION ANALYSIS THE OPTIMAL SOLUTION

We now consider all the cases of the optimal solution with the constrains, especially the constraints (9b) and (9c).

Case I: Assume that the optimal solution is located out of the feasible region of Constraint (9c). In other words, the optimal EE can not satisfy Constraint (9c). In this case, from the trade-off between EE and spectral efficiency, the achievable maximum EE is located at the boundary of feasible region of Constraint (9c). In other words, we have $\frac{2}{T}\int_0^{\frac{T}{2}} C(t)\mathrm{d}t = u$. Then, the objective function in (9a) becomes

$$\max_{P(t)} \frac{uT/2}{\int_0^{\frac{T}{2}} P(t)\mathrm{d}t + P_c}, \tag{31}$$

where the numerator is constant with respect to variable $P(t)$. The optimization problem (9a)-(9d) is equivalent to a average power minimization problem as

$$\begin{aligned} &\min_{P(t)} \int_0^{\frac{T}{2}} P(t)\mathrm{d}t \\ &\text{s.t. (9b), (9d),} \\ &\quad \frac{2}{T}\int_0^{\frac{T}{2}} C(t)\mathrm{d}t = u. \end{aligned} \tag{32}$$

From Appendix A, we obtain the optimal power allocaiton as follows.

In the first phase, $0 \le t \le t_1$, the power allocation can be expressed as

$$P_1^{\text{C-out}}(t) = \frac{2N_0^2}{(1+\lambda)A(t)}\left(\Theta_1^{\text{C-out}}(t) + \sqrt{(\Theta_1^{\text{C-out}}(t))^2 - \Phi_1^{\text{C-out}}(t) + \Omega_1^{\text{C-out}}(t)}\right), \tag{33}$$

where

$$\Theta_1^{\text{C-out}}(t) = \frac{(\eta+\kappa)A(t) - (1+\lambda)B(t)N_0\ln 2}{2N_0^2\ln 2}, \tag{34}$$

$$\Phi_1^{\text{C-out}}(t) = \frac{A(t)(1+\lambda)^2}{N_0^2}, \tag{35}$$

$$\Omega_1^{\text{C-out}}(t) = \frac{(1+\lambda)(\eta+\kappa)A(t)B(t)}{2N_0^3\ln 2}. \tag{36}$$

For the second phase, $t_1 < t \le t_2$, the power allocation can be expressed as

$$P_2^{\text{C-out}}(t) = \max\left\{P_{th}(t), \frac{2N_0^2}{(1+\lambda)A(t)}\left(\Theta_2^{\text{C-out}}(t) + \sqrt{(\Theta_2^{\text{C-out}}(t))^2 - \Phi_1^{\text{C-out}}(t) + \Omega_2^{\text{C-out}}(t)}\right)\right\}, \tag{37}$$

where P_{th} is given by (25), and

$$\Theta_2^{\text{C-out}}(t) = \frac{\eta A(t) - (1+\lambda)B(t)N_0\ln 2}{2N_0^2\ln 2}, \tag{38}$$

$$\Omega_2^{\text{C-out}}(t) = \frac{(1+\lambda)\eta A(t)B(t)}{2N_0^3\ln 2}. \tag{39}$$

The optimal power allocation for the third phase is $P_3^{\text{C-out}}(t) = P_1^{\text{C-out}}(t),\ t_2 < t \le \frac{T}{2}$.

In conclusion, the optimal power allocation scheme for Case I is

$$P^{\text{C-out}*}(t) = \begin{cases} P_1^{\text{C-out}}(t), & 0 \le t \le t_1, \\ P_2^{\text{C-out}}(t), & t_1 < t \le t_2, \\ P_3^{\text{C-out}}(t), & t_2 < t \le \dfrac{T}{2}. \end{cases} \tag{40}$$

We can see from (40) that no auxiliary parameter r needs to be computed iteratively. In this case, outer iteration is not needed.

Case II: Assume that the optimal solution is located out of the feasible region of maximum power constraint (9b). That is, the optimal EE can not satisfy Constraint(9b). In this case, from the trade-off between EE and spectral efficiency, the achievable maximum EE is located at the boundary of feasible region of maximum power constraint. In other words, we have $\frac{2}{T}\int_0^{\frac{T}{2}} P(t)\mathrm{d}t = P_{max}$. Then, the objective function in (9a) becomes

$$\max_{P(t)} \frac{\int_0^{\frac{T}{2}} C(t)\mathrm{d}t}{2P_{max}/T + P_c}, \tag{41}$$

where the denominator is constant. The optimization problem (9a)-(9d) is equivalent to a average rate maximization problem as

$$\begin{aligned} &\max_{P(t)} \int_0^{\frac{T}{2}} C(t)\mathrm{d}t \\ &\text{s.t. (9c), (9d),} \end{aligned}$$

$$\frac{2}{T}\int_0^{\frac{T}{2}} P(t)\mathrm{d}t = P_{max}. \tag{42}$$

From Appendix B, we have the optimal power allocation as follows.

For the first phase, $0 \le t \le t_1$, the power allocation is

$$P_1^{\text{P-out}}(t) = \frac{2N_0^2}{\lambda A(t)}\left(\Theta_1^{\text{P-out}}(t) + \sqrt{(\Theta_1^{\text{P-out}}(t))^2 - \Phi_1^{\text{P-out}}(t) + \Omega_1^{\text{P-out}}(t)}\right), \tag{43}$$

where

$$\Theta_1^{\text{P-out}}(t) = \frac{(1+\eta+\kappa)A(t) - \lambda B(t)N_0 \ln 2}{2N_0^2 \ln 2}, \tag{44}$$

$$\Phi_1^{\text{P-out}}(t) = \frac{A(t)\lambda^2}{N_0^2}, \tag{45}$$

$$\Omega_1^{\text{P-out}}(t) = \frac{\lambda(1+\eta+\kappa)A(t)B(t)}{2N_0^3 \ln 2}. \tag{46}$$

For the second phase, $t_1 < t \le t_2$, the power allocation is

$$P_2^{\text{P-out}}(t) = \max\left\{P_{th}(t),\ \frac{2N_0^2}{\lambda A(t)}\left(\Theta_2^{\text{P-out}}(t) + \sqrt{(\Theta_2^{\text{P-out}}(t))^2 - \Phi_1^{\text{P-out}}(t) + \Omega_2^{\text{P-out}}(t)}\right)\right\}, \tag{47}$$

where P_{th} is also given by (25), and

$$\Theta_2^{\text{P-out}}(t) = \frac{(1+\eta)A(t) - \lambda B(t)N_0 \ln 2}{2N_0^2 \ln 2}, \tag{48}$$

$$\Omega_2^{\text{P-out}}(t) = \frac{(1+\eta)\lambda A(t)B(t)}{2N_0^3 \ln 2}. \tag{49}$$

The optimal power allocation for the third phase is $P_3^{\text{P-out}}(t) = P_1^{\text{P-out}}(t),\ t_2 < t \le \frac{T}{2}$.

In conclusion, the optimal power allocation in Case-I is

$$P^{\text{P-out}*}(t) = \begin{cases} P_1^{\text{P-out}}(t), & 0 \le t \le t_1, \\ P_2^{\text{P-out}}(t), & t_1 < t \le t_2, \\ P_3^{\text{P-out}}(t), & t_2 < t \le \dfrac{T}{2}. \end{cases} \tag{50}$$

We can see from (50) that no auxiliary parameters r needs to be computed iteratively. Similarly to Case I, outer iteration is also not needed in this case.

Case III: Assume that the optimal solution is located in the feasible regions of maximum power and minimum rate. In this case, the optimal EE can always satisfy Constraint (9b) and Constraint (9c). The original problem is equivalent to a optimization problem without these two constraints as

$$\max_{P(t)} \frac{\int_0^{\frac{T}{2}} C(t)\mathrm{d}t}{\int_0^{\frac{T}{2}} P(t)\mathrm{d}t + P_c} \quad \text{s.t.} \int_0^{t_1}(u - C(t))\mathrm{d}t + \int_{t_2}^{\frac{T}{2}}(u - C(t))\mathrm{d}t \le \frac{Q_m}{2}. \tag{51}$$

We can transform this optimization problem by a similar method used in Section III into

$$\max_{P(t)} \int_0^{\frac{T}{2}} C(t)\mathrm{d}t - r\left(\int_0^{\frac{T}{2}} P(t)\mathrm{d}t + P_c\right) \quad \text{s.t.} \int_0^{t_1}(u - C(t))\mathrm{d}t + \int_{t_2}^{\frac{T}{2}}(u - C(t))\mathrm{d}t \le \frac{Q_m}{2}. \tag{52}$$

The optimal solution can be obtained by (27) with the Lagrangian multipliers corresponding to the maximum power constraint and minimum rate constraint being zeros, i.e.,

$$P^{\text{IN}*}(t) = P^{\text{OPT}*}(t)|_{\lambda=0,\eta=0}, \quad 0 \le t \le \frac{T}{2}. \tag{53}$$

Lagrangian multipliers λ and η do not need to be computed iteratively, although the outer iterations still exist in this case.

B. LOW-COMPLEXITY ALGORITHM FOR ENERGY-EFFICIENT POWER ALLOCATION

We have discussed all the cases of the optimal solution in feasible region in the above subsection. In any of the above cases, we can solve the optimization problem with a lower complexity. However, before solving the original problem (9a)-(9d), we generally do not know which case the optimal solution belongs to.

For convenience, we denote $f_R = \int_0^{\frac{T}{2}} C(t)\mathrm{d}t$ and $f_P = \int_0^{\frac{T}{2}} P(t)\mathrm{d}t + P_c$. According to (30), we have $F(r) = \max_{P(t)}\{f_R - rf_P\}$. From [37], [40], the optimal solution of (9a)-(9d) is obtained at

$$\begin{aligned} F(r^*) &= \max_{P(t)}\{f_R(P(t)) - r^* f_P(P(t))\} \\ &= f_R(P^*(t)) - r^* f_P(P^*(t)) = 0. \end{aligned} \tag{54}$$

The optimization problem (10) can be regard as a multi-objective optimization problem where f_R is to be maximized while f_P is to be minimized. And the optimal power $P^*(t)$ in (27) is a Pareto-optimal solution for an r. The set of these Pareto optimal values is called the optimal trade-off curve between the two objectives, as shown in Fig. 3. The parameter r is the slope of the trade-off curve, i.e. $\frac{f_R}{f_P}$, and $F(r)$ is the intersection of the tangent with the vertical axis. The point of tangency is Pareto optimal solution $P(t)$, and the global optimal r^* is obtained at $F(r^*) = 0$.

To derive a low-complexity algorithm, we analysis the upper and lower bounds in the bisection method and find the relationship between the optimal solution and the bounds. From Fig. 3, we can see that $f_R(P^{(n)}(t))$ with iteration index n is monotonically decreasing with the updated lower bound of r_d. In other words, if $f_R(P^{(n)}(t))$ does not satisfy (9c), neither do $f_R(P^{(n+1)}(t))$ and the optimal $f_R(P^*(t))$, i.e.,

$$\begin{aligned} \frac{2}{T}f_R(P^{(n)}(t)) < u &\Rightarrow \frac{2}{T}f_R(P^{(n+1)}(t)) < u \\ &\Rightarrow \frac{2}{T}f_R(P^*(t)) < u. \end{aligned} \tag{55}$$

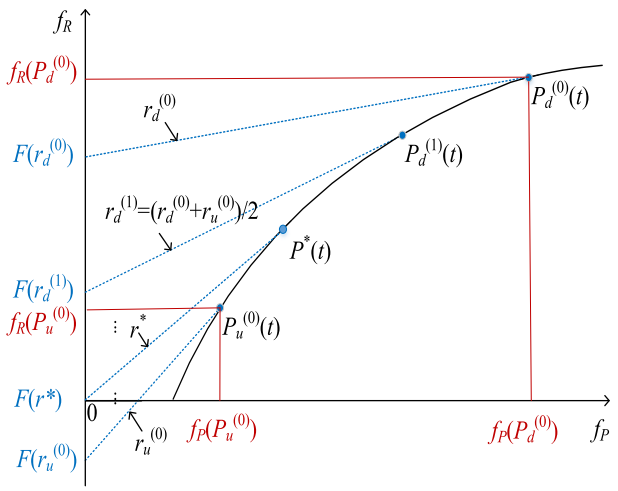

FIGURE 3. The optimal trade-off curve between f_R and f_P.

In addition, we can see that $f_P(P^{(n)}(t))$ with iteration index n is monotonically increasing with the updated upper bound of r_u. In other words, if $f_P(P^{(n)}(t))$ does not satisfy (9d), neither do $f_P(P^{(n+1)}(t))$ and the optimal $f_P(P^*(t))$, i.e.,

$$\begin{aligned}&\frac{2}{T}(f_P(P^{(n)}(t))-P_C)>P_{max}\\&\Rightarrow\frac{2}{T}(f_P(P^{(n+1)}(t))-P_C)>P_{max}\\&\Rightarrow\frac{2}{T}(f_P(P^*(t))-P_C)>P_{max}.\end{aligned}\tag{56}$$

Based on the above discussions, we propose a low-complexity algorithm for maximizing EE in HSR communciations, as shown in Algorithm 2.

Algorithm 2 Low-Complexity EE Power Allocation Algorithm in HSR Communications With Buffer Constraint

Initialization

1. Initialize tolerance ε and index $n=1$.
2. Initialize $r_d^{(0)}$ and $r_u^{(0)}$ with $F(r_d^{(0)})>0$ and $F(r_u^{(0)})<0$.

Iterative Algorithm

3. **while**
4. Update r by $r^{(n)}=(r_d^{(n-1)}+r_u^{(n-1)})/2$.
5. Compute $P^{(n)}(t)$ for the given $r^{(n)}$ by $P^{\mathrm{IN}*}(t)$ in (53).
6. **if** $F(r^{(n)})>0$
7. Update $r_d^{(n)}=r^{(n)}$ and $r_u^{(n)}=r_u^{(n-1)}$.
8. **if** $\frac{2}{T}\int_0^{\frac{T}{2}}C(t)\mathrm{d}t<u$
9. Go to step 17.
10. **endif**
11. **else**
12. Update $r_d^{(n)}=r_d^{(n-1)}$ and $r_u^{(n)}=r^{(n)}$.
13. **if** $\frac{2}{T}\int_0^{\frac{T}{2}}P(t)\mathrm{d}t>P_{max}$
14. Go to step 18.
15. **endif**
16. **endif**
17. Set $n=n+1$.
18. **endwhile** converge to the optimal $P^*(t)$ with ε.
19. Compute the optimal $P^*(t)$ by $P^{\text{C-out}*}$ in (40).
20. Compute the optimal $P^*(t)$ by $P^{\text{P-out}*}$ in (50).

V. SIMULATION RESULTS AND DISCUSSIONS

Numerical simulation results are presented in this section to evaluate the performance of the proposed low-complexity energy-efficient power allocation in HSR communications with buffer constraint. The advantages of the proposed algorithm are mainly reflected in two aspects. First, the proposed algorithm can reduce the complexity of traditional bisection method without degrading system performance. Second, the proposed algorithm can meet the buffer constraint by comparing several conventional power allocation methods. Note that the common simulation parameters [9], [33], [35], [36], are listed in Table 1.

TABLE 1. Parameter settings.

Parameter	Description	Value
v	speed of the train	100 m/s
α	path loss exponent	3.6
d_v	vertical distance	50 m
d_r	distance between MRs	400 m
d_h	distance between RAUs	1000 m
Q_m	buffer size	4 bits/Hz
u	data arrival rate	8 bits/s/Hz
P_{ave}	average transmit power	40 W
N_0	noise power	10^{-9} W/Hz

A. ENERGY EFFICIENCY AND ITERATION PERFORMANCE

Fig. 4 shows the EE performance of the proposed algorithms versus the minimum data rate requirements of the system. In this figure, we also consider the water-filling algorithm and channel inversion algorithm as comparisons. We can see that the proposed optimal method based on bisection algorithm (i.e., Algorithm 1) can achieve the highest EE performance. And the low-complexity algorithm (i.e., Algorithm 2) has a same EE performance with bisection algorithm, and is superior to the water-filling and channel inversion algorithms. In addition, except for the water-filling method, the achievable EE decreases with the increase of data arrival rate. This is because that more power should be consumed to guarantee the transmission of arrival data, which narrows the feasible region of the solution and results in a lower EE. The performance of water-filling method keeps invariable with increasing u since it always aims at the maximum data-rate. Moreover, we also see that as the fixed circuit power consumption P_c increases, the EE performance decreases.

Fig. 5 shows the EE performance of the proposed algorithm versus the maximum transmit power of the RAUs. Similar to the data arrival rate requirements, the optimal EE can be achieved when the maximum of transmit power P_{max} allowed by the RAUs is large enough. The EE that can be achieved increases with the increases of P_{max} when the maximum transmit power limitation of the RAUs can not meet the optimal EE. Therefore, the reduction of algorithm complexity

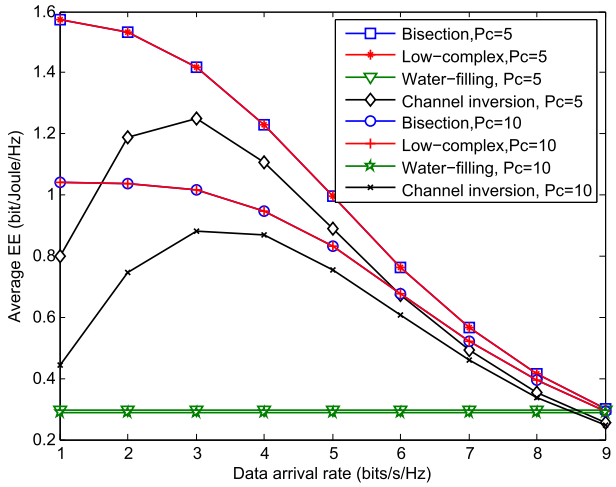

FIGURE 4. Average EE versus the minimum data rate requirement of the system.

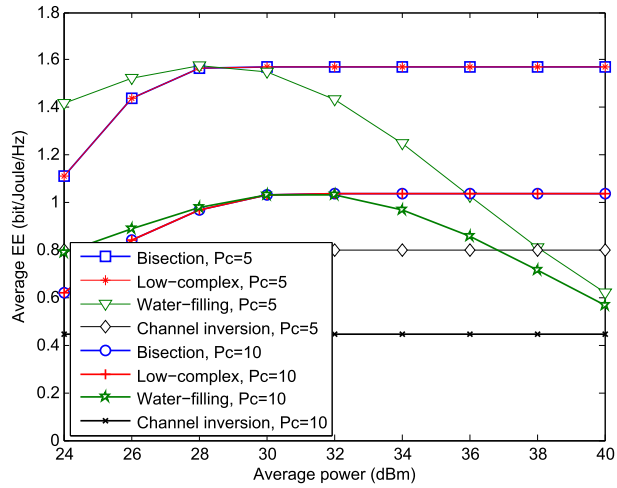

FIGURE 5. Average EE versus the maximum transmit power of the RAUs.

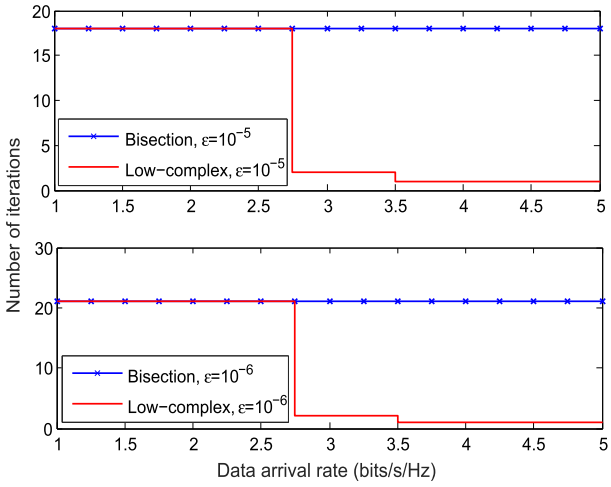

FIGURE 6. Average number of iterations versus the minimum data rate requirement of the system.

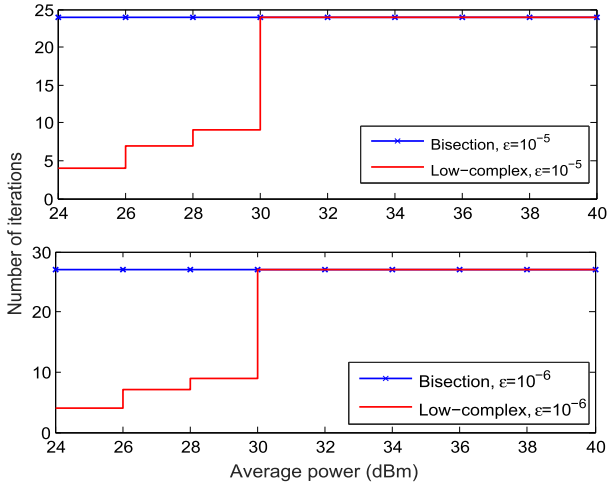

FIGURE 7. Average number of iterations versus the maximum transmit power of the RAUs.

does not bring the loss of EE performance, which shows the effectiveness of the proposed low-complexity algorithm. Furthermore, the proposed algorithms (i.e., bisection algorithm and low-complexity algorithm) can achieve the highest EE when maximum power is large. The water-filling method can not satisfy the buffer limitation, although it has a higher EE when transmit power is small. The channel inversion method is limited by the arrival data rate and its EE keeps invariable with increasing P_{max}.

Fig. 6 depicts the iterations of the proposed algorithms over different data arrival rate requirements. It can be seen that the low-complexity algorithm can greatly reduce the iterations, especially when the rate requirement is really strict. As the data rate requirement increases, the iteration of low-complexity algorithm decreases. This is because that the rate constraint is more difficult to be satisfied when it becomes strict, which leads to jumping out of the loop and ending of the iteration process. Additionally, as the requirement of convergence accuracy increases, the disadvantage of bisection algorithm is more obvious since the larger number of iteration is needed.

Fig. 7 shows the iterations versus the maximum of transmit power allowed P_{max} by the RAUs. It shows that, as the P_{max} decreases, the number of iterations decreases. This is due to that when the power constraint becomes strict, they are more difficult to be satisfied, which leads to jumping out of the loop and ending of the iteration process. More importantly, the proposed algorithm not only reduces iterations, but also reduces the constraints to be solved in each iteration. However, traditional methods need to solve more constraints of optimization.

Note that, combining the results in Fig. 6 and Fig. 7, we get that when both the transmit power limitation and data rate requirement exist, the iteration number of low-complexity algorithm is the smallest one of that for the two constraints. On the other hand, we also see that when the two constraints

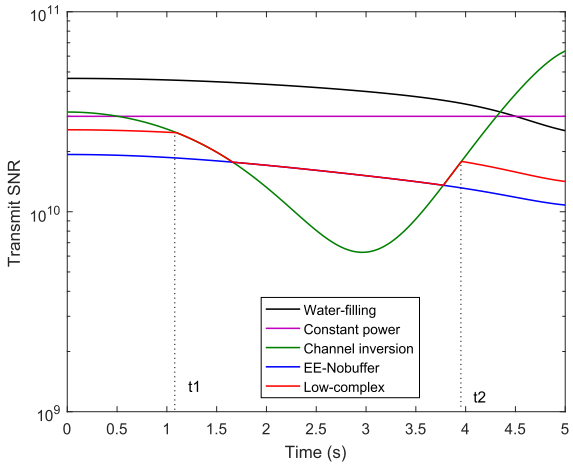

FIGURE 8. Transmit SNR versus time at RAUs under different power allocation schemes.

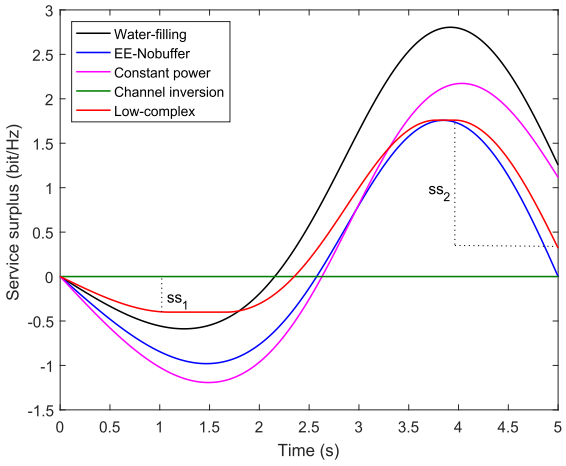

FIGURE 10. Service surplus versus data arrival rate under different schemes.

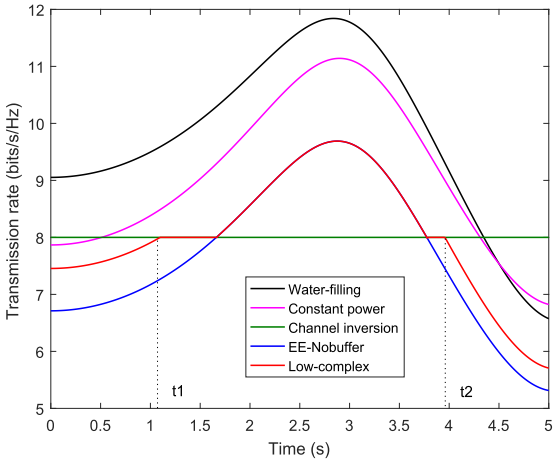

FIGURE 9. Instantaneous transmission rate versus time at RAUs under different power allocation schemes.

are not strict (i.e., smaller data rate requirement or larger transmit power), the iteration number of the low-complexity method is the same with the bisection method. However, in this case, the bisection method needs inner iterations to update the Lagrange multipliers corresponding to the two constraints, but the low-complexity algorithm needs not do it. That is, the low-complexity method has a lower computing complexity than bisection method, and gets the optimal EE performance.

B. BUFFER AND DELAY PERFORMANCES

To demonstrate the effectiveness of the proposed power allocation method more clearly, we provide some performance results versus time in Fig. 8. We also give the results of constant power allocation method and energy-efficient method without considering buffer constraint. As shown in this figure, for a given buffer size, the low-complexity energy-efficient power allocation is actually divided into five parts. The water-filling method with a certain water level is adopted in the first part from 0 to 1.11s and the final part from 3.96s to 5s. The channel inversion is adopted in the second part from 1.11s to 1.51s and the fourth part 3.77s to 3.96s. The energy-efficient method without considering buffer constraint is adopted in the third part from 1.51s to 3.77s.

Fig. 9 shows the wireless transmission rate over time under four different schemes. According to observation, we can see the combination of water-filling algorithm, channel inversion method and EE without buffer method more intuitively. From (27), we have known that the power allocation is divided into three phases. In Fig. 8 and Fig. 9, we can see $t_1 = 1.11$ and $t_2 = 3.96$. The two figure also show that the power allocation in $t_1 < t \leq t_2$ is further divided into three part. This is because the optimal power allocation should guarantee $C(t)$ is large than u in this period of time according to (24).

Fig. 10 illustrates the change in service surplus (SS) over time of our proposed scheme compared to water-filling, channel inversion, constant power and the method without buffer constraint. The SS means the cumulative difference between the wireless transmission rate and the data arrival rate, i.e., $\int_0^t (C(\tau) - u)\mathrm{d}\tau$. In other words, the larger the SS is, the faster the buffer is emptied. Since the SS capability is related to the instantaneous wireless transmission rate of the transmitter, the SS process can also be divided into five parts. For the first part, $C(t)$ is smaller than u, there will be data buffering. Therefore, the SS is negative at the time 0 and will continue to decrease. Next, the SS gradually increases and then decreases as the channel conditions get better first and then worse. Furthermore, the amount of SS decline can be seen as data buffering. As shown in Fig. 10, the maximum amount of buffered data, $ss_1 + ss_2 = 0.40 + 1.44 = 1.84$, which is less than buffer size limitation $\frac{Q_m}{2} = 2$. However, the constant power, water-filling and EE without buffer methods (with maximum amount of buffered data 2.15, 2.07 and 2.73 respectively) would not satisfied the buffer constraint because surplus decline under these three methods surpasses the buffer constraint. In this case, data overflow exists in these methods, which will influence the communication between the CU and the train.

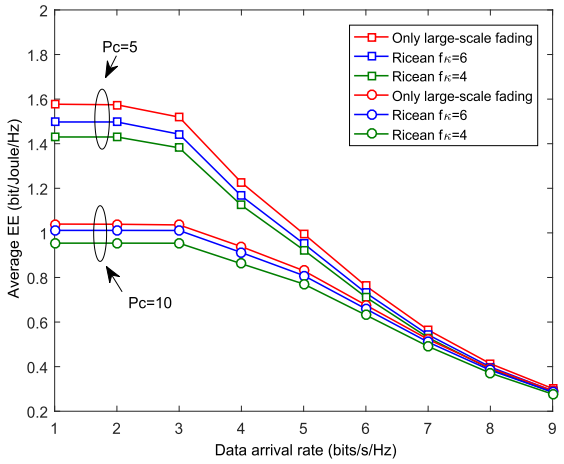

FIGURE 11. Impact of small-scale fading on average EE performance of proposed algorithm.

C. IMPACT OF SMALL-SCALE FADING

In above sections, we designed our work based on the positions of the train without regard to the small-scale fading, due to its unpredictability. The main advantage of this desgin is that no channel estimation is required in our algorithm with an almost uniform movement speed of the train.

Here, we test the performance of the proposed algorithm under the practical channel condition with both path loss and Rician fading (i.e., small-scale fading). In the simulation, we consider different Rician factors $f\kappa$, which denotes the ratio of line-of-sight (LOS) signal power and multi-path component power. From Fig. 11, we can see that the small-scale fading degrades the EE performance. This is because that our algorithm is designed based on only the pass loss and has some performance penalty under the small-scale fading. However, it is worth noting that the achievable average EE is closer to the performance with only large-scale fading when $f\kappa$ is large (i.e., strong LOS). Fortunately, the HSR scenario is just such an environment with the strong LOS, especially the viaduct scenarios.

VI. CONCLUSION

In this paper, two energy-efficient power allocation methods are studied for DAS in HSR communications with data buffer constraint. First, we analyze the relationship between the data arrival rate and wireless transmission rate at RAUs by taking constant power transmitted as an example. Then, we formulate the non-convex power allocation optimization problem and solve it by two iterative algorithms, i.e., the optimal algorithm based on bisection method and the low-complexity algorithm based on feasible domain of the solution. Simulation results have demonstrated the superiority of proposed power allocation scheme. Compared to existing methods, the proposed power allocation schemes can achieve the optimal EE and avoid data overflow. Particularly, in the proposed low-complexity scheme, the reduction of algorithm complexity does not bring any loss of EE performance. In the future, small-scale fading should be considered in the design of power allocation algorithm.

APPENDIX A

The optimization problem in (32) is convex, and the corresponding Lagrangian function is given by

$$\begin{aligned}&\mathcal{L}^{\text{C-out}}(P(t),\lambda,\eta,\kappa)\\&=\int_0^{\frac{T}{2}}P(t)\mathrm{d}t+\lambda\int_0^{\frac{T}{2}}(P(t)-P_{ave})\mathrm{d}t\\&\quad-\eta\int_0^{\frac{T}{2}}(C(t)-u)\mathrm{d}t-\kappa\int_0^{t_1}(C(t)-u+\frac{Q_m}{2t_1})\mathrm{d}t\\&\quad-\kappa\int_{t_2}^{\frac{T}{2}}(C(t)-u+\frac{Q_m}{T-2t_2})\mathrm{d}t.\end{aligned}\tag{57}$$

For the first phase, $0\le t\le t_1$, we have

$$\mathcal{L}_1^{\text{C-out}}=(1+\lambda)\int_0^{t_1}P(t)\mathrm{d}t-(\eta+\kappa)\int_0^{t_1}C(t)\mathrm{d}t+Cons.\tag{58}$$

Deriving (58) with respect to $P(t)$, we have

$$\frac{\partial\mathcal{L}_1^{\text{C-out}}}{\partial P(t)}=1+\lambda-(\eta+\kappa)\frac{\partial C(t)}{\partial P(t)}=0,\tag{59}$$

where $\frac{\partial C(t)}{\partial P(t)}$ is given by (14). Thus, we obtain the power allocation $P_1^{\text{C-out}}(t)$ as (33).

Then, for the second phase, $t_1<t\le t_2$, we get

$$\mathcal{L}_2^{\text{C-out}}=(1+\lambda)\int_{t_1}^{t_2}P(t)\mathrm{d}t-\eta\int_{t_1}^{t_2}C(t)\mathrm{d}t+Cons.\tag{60}$$

Deriving (60) with respect to $P(t)$, we have

$$\frac{\partial\mathcal{L}_2}{\partial P(t)}=1+\lambda-\eta\frac{\partial C(t)}{\partial P(t)}=0.\tag{61}$$

Because $C(t)\ge u$ for $t_1<t\le t_2$, the power allocation $P_2^{\text{C-out}}(t)$ in the second phase can be given by (37). The optimal power allocation in the third phase is similar to the first phase, so we have $P_3^{\text{C-out}}(t)=P_1^{\text{C-out}}(t),\ t_2<t\le\frac{T}{2}$.

APPENDIX B

The optimization problem in (42) is also convex, and the corresponding Lagrangian function is

$$\begin{aligned}&\mathcal{L}^{\text{P-out}}(P(t),\lambda,\eta,\kappa)\\&=-\int_0^{\frac{T}{2}}C(t)\mathrm{d}t+\lambda\int_0^{\frac{T}{2}}(P(t)-P_{ave})\mathrm{d}t\\&\quad-\eta\int_0^{\frac{T}{2}}(C(t)-u)\mathrm{d}t-\kappa\int_0^{t_1}(C(t)-u\mathrm{d}t\\&\quad-\kappa\int_{t_2}^{\frac{T}{2}}(C(t)-u+\frac{Q_m}{T-2t_2})\mathrm{d}t.\end{aligned}\tag{62}$$

For the first phase, $0\le t\le t_1$, we have

$$\mathcal{L}_1^{\text{P-out}}=-(1+\eta+\kappa)\int_0^{t_1}C(t)\mathrm{d}t+\lambda\int_0^{t_1}P(t)\mathrm{d}t+Cons.\tag{63}$$

Deriving (63) with respect to $P(t)$, we have

$$\frac{\partial \mathcal{L}_1^{\text{P-out}}}{\partial P(t)} = \lambda - (1+\eta+\kappa)\frac{\partial C(t)}{\partial P(t)} = 0, \quad (64)$$

where $\frac{\partial C(t)}{\partial P(t)}$ is given by (14). We can obtain $P_1^{\text{P-out}}(t)$ in (43).

Then, for the second phase, $t_1 < t \leq t_2$, we get

$$\mathcal{L}_2^{\text{P-out}} = -(1+\eta)\int_{t_1}^{t_2} C(t)\mathrm{d}t + \lambda \int_{t_1}^{t_2} P(t)\mathrm{d}t + Cons. \quad (65)$$

Deriving (65) with respect to $P(t)$, it can be found

$$\frac{\partial \mathcal{L}_2}{\partial P(t)} = \lambda - (1+\eta)\frac{\partial C(t)}{\partial P(t)} = 0. \quad (66)$$

Because $C(t) \geq u$ for $t_1 < t \leq t_2$, we obtain $P_2^{\text{P-out}}(t)$ in (47). The optimal power allocation for the third phase is similar to the first phase, so we have $P_3^{\text{P-out}}(t) = P_1^{\text{P-out}}(t),\ t_2 < t \leq \frac{T}{2}$.

REFERENCES

[1] R. He, G. Wang, K. Guan, Z. Zhong, A. F. Molisch, C. Briso-Rodriguez, and C. P. Oestges, "High-speed railway communications: From GSM-R to LTE-R," *IEEE Veh. Technol. Mag.*, vol. 11, no. 3, pp. 49–58, Sep. 2016.

[2] A. Kumar, K. Singh, and D. Bhattacharya, "Green communication and wireless networking," in *Proc. ICGCE*, 2013, pp. 49–52.

[3] I. Chih-Lin, C. Rowell, S. Han, Z. Xu, G. Li, and Z. Pan, "Toward green and soft: A 5G perspective," *IEEE Commun. Mag.*, vol. 52, no. 2, pp. 66–73, Feb. 2014.

[4] J. Huang and Z. Zhong, "Dynamic green communication strategy for railway cellular network," in *Proc. IEEE VTC Spring*, May 2014, pp. 1–5.

[5] Z. Wang, "Green design and humanized design in high speed train's industrial design management," in *Proc. Int. Conf. Manage. Service Sci.*, Aug. 2011, pp. 1–3.

[6] Z. He, Z. Yang, and J. Lv, "An energy-efficient operation strategy for high-speed trains," in *Proc. Chin. Control Decision Conf.*, 2018, pp. 3771–3776.

[7] L. Wang, B. Ai, Y. Niu, X. Chen, and P. Hui, "Energy-efficient power control of train-ground mmWave communication for high speed trains," *IEEE Trans. Veh. Technol.*, to be published. doi: 10.1109/TVT.2019.2923066.

[8] J. Wu and P. Fan, "A survey on high mobility wireless communications: Challenges, opportunities and solutions," *IEEE Access*, vol. 4, pp. 450–476, 2016.

[9] S. Li, G. Zhu, S. Lin, Q. Gao, S. Xu, and L. Xiong, "Energy-efficient power allocation in cloud radio access network of high-speed railway," in *Proc. IEEE VTC Spring*, May 2016, pp. 1–5.

[10] J. D. O. Sanchez and J. I. Alonso, "A two-hop MIMO relay architecture using LTE and millimeter wave bands in high-speed trains," *IEEE Trans. Veh. Technol.*, vol. 68, no. 3, pp. 2052–2065, Mar. 2019.

[11] K. Xiong, P. Fan, Y. Zhang, and K. B. Letaief, "Towards 5G high mobility: A fairness-adjustable time-domain power allocation approach," *IEEE Access*, vol. 5, pp. 11817–11831, Jun. 2017.

[12] T. Li, K. Xiong, P. Fan, and K. B. Letaief, "Service-oriented power allocation for high-speed railway wireless communications," *IEEE Access*, vol. 5, pp. 8343–8356, May 2017.

[13] I. Ahmad, W. Chen, and K. Chang, "LTE-railway user priority-based cooperative resource allocation schemes for coexisting public safety and railway networks," *IEEE Access*, vol. 5, pp. 7985–8000, May 2017.

[14] J. Qiu, Z. Lin, W. Hardjawana, B. Vucetic, C. Tao, and Z. Tan, "Resource allocation for OFDMA system under high-speed railway condition," in *Proc. IEEE WCNC*, Apr. 2014, pp. 2683–2687.

[15] C. Zhang and P. Fan, "Providing servises for the high-speed train and local users in the same OFDMA system: Resource allocation in the downlink," *IEEE Trans. Wireless Commun.*, vol. 15, no. 2, pp. 1018–1030, Feb. 2016.

[16] Z. Sheng, H. D. Tuan, Y. Fang, H. H. M. Tam, and Y. Sun, "Data rate maximization based power allocation for OFDM System in a high-speed train environment," in *Proc. IEEE GlobalSIP*, Dec. 2015, pp. 265–269.

[17] Q. Gao, G. Zhu, S. Lin, S. Li, L. Xiong, W. Xie, and X. Qiao, "Robust QoS-aware cross-layer design of adaptive modulation transmission on OFDM systems in high-speed railway," *IEEE Access*, vol. 4, pp. 7289–7300, 2016.

[18] H. Ghazzai, T. Bouchoucha, A. Alsharoa, E. Yaacoub, and M.-S. Alouini, "Transmit power minimization and base station planning for high-speed trains with multiple moving relays in OFDMA systems," *IEEE Trans. Veh. Technol.*, vol. 66, no. 1, pp. 175–187, Jan. 2017.

[19] Y. Zhao, X. Li, X. Zhang, Y. Li, and H. Ji, "Multidimensional resource allocation strategy for high-speed railway MIMO-OFDM system," in *Proc. IEEE GLOBECOM*, Dec. 2012, pp. 1653–1657.

[20] Y. Zhao, X. Li, Y. Li, and H. Ji, "Resource allocation for high-speed railway downlink MIMO-OFDM system using quantum-behaved particle swarm optimization," in *Proc. IEEE ICC*, Jun. 2013, pp. 2343–2347.

[21] Y. Lu, K. Xiong, P. Fan, and Z. Zhong, "Optimal multicell coordinated beamforming for downlink high-speed railway communications," *IEEE Trans. Veh. Technol.*, vol. 66, no. 10, pp. 9603–9608, Oct. 2017.

[22] X. Liu and D. Qiao, "Location-fair beamforming for high speed railway communication systems," *IEEE Access*, vol. 6, pp. 28632–28642, May 2018.

[23] K. Xu, Z. Shen, Y. Wang, and X. Xia, "Location-aided mMIMO channel tracking and hybrid beamforming for high-speed railway communications: An angle-domain approach," *IEEE Syst. J.* to be published. doi: 10.1109/JSYST.2019.2911296.

[24] Y. Ge, W. Zhang, F. Gao, S. Zhang, and X. Ma, "Beamforming network optimization for reducing channel time variation in high-mobility massive MIMO," *IEEE Trans. Commun.*, to be published. doi: 10.1109/TCOMM.2019.2926464.

[25] X. You, D. Wang, P. Zhu, and B. Sheng, "Cell edge performance of cellular mobile systems," *IEEE J. Sel. Areas Commun.*, vol. 29, no. 6, pp. 1139–1150, Jun. 2011.

[26] J. Wang, H. Zhu, and N. J. Gomes, "Distributed antenna systems for mobile communications in high speed trains," *IEEE J. Sel. Areas Commun.*, vol. 30, no. 4, pp. 675–683, May 2012.

[27] H. Wang, H. Hou, and J. Chen, "Design and analysis of an antenna control mechanism for time division duplexing distributed antenna systems over high-speed rail communications," *IEEE Trans. Emerg. Topics Comput.*, vol. 4, no. 4, pp. 516–527, Oct./Dec. 2016.

[28] S. Xu, G. Zhu, B. Ai, and Z. Zhong, "A survey on high-speed railway communications: A radio resource management perspective," *Comput. Commun.*, vol. 86, pp. 12–28, Apr. 2016.

[29] C. He, B. Sheng, P. Zhu, and X. You, "Energy efficiency and spectral efficiency tradeoff in downlink distributed antenna systems," *IEEE Wireless Commun. Lett.*, vol. 1, no. 3, pp. 153–156, Jun. 2012.

[30] C. He, G. Y. Li, F.-C. Zheng, and X. You, "Power allocation criteria for distributed antenna systems," *IEEE Trans. Veh. Technol.*, vol. 64, no. 11, pp. 5083–5090, Nov. 2015.

[31] Z. Liu and P. Fan, "An effective handover scheme based on antenna selection in ground-train distributed antenna systems," *IEEE Trans. Veh. Technol.*, vol. 63, no. 7, pp. 3342–3350, Sep. 2014.

[32] J. Lu, K. Xiong, X. Chen, and P. Fan, "Toward traffic patterns in high-speed railway communication systems: Power allocation and access selection," *IEEE Trans. Veh. Technol.*, vol. 67, no. 12, pp. 12273–12287, Dec. 2018.

[33] J. Hu, X. Wang, and Y. Xu, "Energy-efficient power optimization and transmission mode selection for distributed antenna system in HSR communications," in *Proc. IEEE Veh. Technol. Conf.*, Apr. 2019, pp. 1–5.

[34] M. Zafer and E. Modiano, "Optimal rate control for delay-constrained data transmission over a wireless channel," *IEEE Trans. Inf. Theory*, vol. 54, no. 9, pp. 4020–4039, Sep. 2008.

[35] C. Zhang, P. Fan, K. Xiong, and P. Fan, "Optimal power allocation with delay constraint for signal transmission from a moving train to base stations in high-speed railway scenarios," *IEEE Trans. Veh. Technol.*, vol. 64, no. 12, pp. 5775–5788, Dec. 2015.

[36] M. Yu, X. Wang, Y. Xu, D. Li, and J. Chen, "Energy-efficient power allocation with buffer constraint for high-speed railway," in *Proc. IEEE ICCS*, Dec. 2018, pp. 343–347.

[37] X. Wang, F.-C. Zheng, P. Zhu, and X. You, "Energy-efficient resource allocation in coordinated downlink multicell OFDMA systems," *IEEE Trans. Veh. Technol.*, vol. 65, no. 3, pp. 1395–1408, Mar. 2016.

[38] S. Ali, A. Ahmad, and A. Khan, "Energy-efficient resource allocation and RRH association in multitier 5G H-CRANs," *Trans. Emerg. Telecommun. Technol.*, vol. 30, no. 1, pp. 1–15, Jan. 2019.

[39] S. Boyd and L. Vandenberghe, *Convex Optimization*. Cambridge, U.K.: Cambridge Univ. Press, 2004.

[40] W. Dinkelbach, "On nonlinear fractional programming," *Manage. Sci.*, vol. 13, no. 7, pp. 492–498, Mar. 1967. [Online]. Available: http://www.jstor.org/stable/2627691

XIAOMING WANG (M'16) received the Ph.D. degree in information and communication engineering from the National Mobile Communications Research Laboratory, Southeast University, Nanjing, China, in 2016. He is currently a Lecturer with the Nanjing University of Posts and Telecommunications (NJUPT), Nanjing. His research interests include radio resource management, green communications, and machine learning in communications.

MI YU received the B.E. degree in communication engineering from the Anhui University of Technology, Maanshan, China, in 2017. She is currently pursuing the master's degree with the Nanjing University of Posts and Telecommunications (NJUPT), Nanjing, China. Her research interests include high-speed railway communications and radio resource allocation.

JINLING HU received the B.E. degree in communication engineering from Anhui Polytechnic University, Wuhu, China, in 2017. She is currently pursuing the master's degree with the Nanjing University of Posts and Telecommunications (NJUPT), Nanjing, China. Her research interests include high-speed railway communications and massive MIMO systems.

YOUYUN XU (M'02–SM'11) received the Ph.D. degree in information and communication engineering from Shanghai Jiao Tong University (SJTU), China, in 1999. He is currently a Professor with the Nanjing University of Posts and Telecommunications. He is also a part-time Professor with the Institute of Wireless Communication Technologies, SJTU. He has over 20-year professional experience of teaching and researching in communication theory and engineering with research and development achievement, such as the WCDMA Trial System under C3G Framework in China, in 1999, the B3G-TDD Trial System under FuTURE Framework in China, in 2006, and the Chinese Digital TV Broadcasting System. His current research interests include new-generation wireless mobile communication systems (LTE, IM-T Advanced, and related), advanced channel coding and modulation techniques, multiuser information theory and radio resource management, wireless sensor networks, and cognitive radio networks. He is a Senior Member of the Chinese Institute of Electronics and a member of IEICE.